PERGAMON

Scripta Materialia 45 (2001) 245–252

Scripta MATERIALIA

www.elsevier.com/locate/scriptamat

Investigation of thermal residual stresses in tungsten-fiber/bulk metallic glass matrix composites

Danut Dragoi[a*], Ersan Üstündag[a*], Bjorn Clausen[a], and Mark A.M. Bourke[b]

[a]*Department of Materials Science, California Institute of Technology, M/C 138-78 Pasadena, CA 91125, USA*
[b]*Materials Science and Technology Division, Los Alamos National Laboratory, Los Alamos, NM 87545, USA*

Received 6 November 2000; accepted 6 April 2001

Keywords: Metallic glasses; Neutron scattering; Thermal expansion; Shear bands; Non-destructive evaluation

Introduction

Bulk metallic glasses (BMGs) have recently gained popularity due to the development of new alloys that yield a glassy structure even with "conventional" metal processing such as casting [1]. The unique properties of BMGs potentially place them among significant engineering materials: very high strength (1.9 GPa) and fracture toughness (40–55 MPa $m^{1/2}$), a near theoretical specific strength, excellent wear and corrosion resistance, and a high elastic strain limit of up to 2% [2,3].

However one major drawback of BMGs is that they fail catastrophically when unconstrained (e.g., in uniaxial tension) by forming localized shear bands. To avoid this and to obtain more damage tolerance, BMGs are reinforced with fibers or particulates [4–6]. These studies demonstrated that the composite approach could be quite beneficial. The reinforcements interact with the shear bands and obstruct their propagation. Even in high rate dynamic deformation, the presence of reinforcement causes the development of multiple shear bands, thus increasing the amount of strain accommodated by the material prior to failure [5]. Despite these empirically observed improvements, there remain unresolved issues concerning the interaction mechanisms between the shear bands and the reinforcement. In addition, the 'best' reinforcement and its morphology are yet to be identified.

One important issue in BMG matrix composites is the presence of thermal residual stresses due to the mismatch in coefficients of thermal expansion (CTE) between the

* Corresponding authors.
E-mail addresses: ddragoi@cco.caltech.edu (D. Dragoi), ersan@caltech.edu (E. Üstündag).

PII: S1359-6462(01)01031-4

matrix and the reinforcements. Since these stresses are predicted to reach several hundred MPa [4], they are expected to significantly influence the mechanical behavior. For instance, in contrast with most metal–matrix ceramic systems, tensile residual stresses in the reinforcement might be *beneficial* since this will attract cracks (or shear bands) increasing their probability of being blunted or stopped. As part of a systematic study on the interactions between the matrix and reinforcements in BMG composites, this article presents results on the thermal residual stresses/strains in these materials determined by neutron powder diffraction (NPD) and finite element (FE) modeling.

Experimental procedure

Unidirectional tungsten (W) fibers of about 250 μm in diameter, 99.9% purity (from Thermionics Products Co., North Plainfield, NJ), were introduced into a BMG alloy (Vitreloy 1^{TM}:$Zr_{41.2}Ti_{13.8}Cu_{12.5}Ni_{10.0}Be_{22.5}$) in four volume fractions: 20%, 40%, 60% and 80%. Specimens were cylinders of about 50.0 mm in length and 7.75 mm in diameter (aspect ratio, $l/d = 6.5$). Processing was by melt infiltration casting which is described in detail elsewhere [7]. Briefly, the fibers are placed in a quartz-glass tube and then molten BMG alloy is infiltrated among them by applying gas pressure. The tube is then quenched in a brine solution. Loose W fibers that were heat treated under similar conditions were used as "stress-free" reference in residual stress measurements.

The presence of heavy elements such as W, Zr and Ni precludes the use of X-ray diffraction (for most energy ranges) to determine the residual stresses in the W fibers. For this reason, the diffraction experiments were conducted on the neutron powder diffractometer at the Los Alamos Neutron Science Center (LANSCE) using a 10×50 mm^2 neutron beam. For these composites, the penetration depth of neutrons through which the beam intensity drops to $1/e$ is estimated to be on the order of 15 mm allowing the complete sampling of the specimen cross-section. LANSCE employs spallation neutrons and the time-of-flight (TOF) technique, which means that diffraction patterns (for a range of d spacings) are measured simultaneously by, in this case, two detector banks at scattering angles of $\pm 90°$ (Fig. 1). In this arrangement, the $2\theta = -90°$ detector

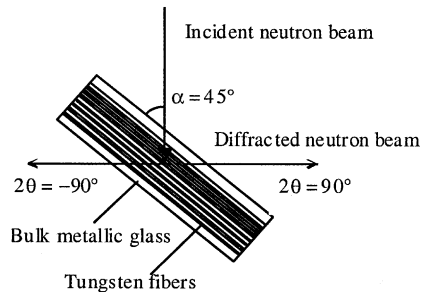

Fig. 1. Schematic of the scattering geometry used. The specimen is oriented at 45° to the incident beam and data are collected by detectors at $\pm 90°$ (2θ).

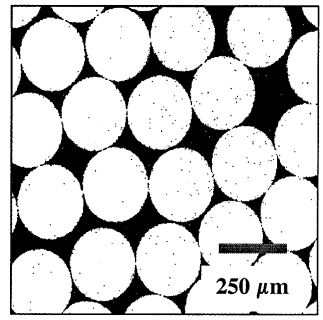

Fig. 2. The scanning electron microscope image of the 80% W/BMG composite (in backscattered electron mode). The dark areas represent the BMG matrix while the light regions show the W fibers.

measures the longitudinal strain while the $2\theta = +90°$ detector determines the transverse strain in the W fibers.

The diffraction data were analyzed using the Rietveld method [8,9]. The following parameters were refined (in order): scale factor; background, lattice parameter, orientation distribution function for texture, absorption, extinction, and isotropic atomic displacements, U_{iso}. All of these parameters are described elsewhere in more detail [10]. The texture analysis was conducted using the spherical harmonic function method [11].

Cross-sections of the specimens were subsequently investigated using scanning electron microscopy and electron microprobe analysis. Some non-uniform distribution of fibers was noted in all specimens (Fig. 2). The microprobe analysis confirmed that no measurable amount of matrix elements dissolved in the W fibers during melt infiltration. This way, the use of heat-treated loose W fibers as "stress-free" reference could be justified.

Finite element modeling

Since there are no sharp diffraction peaks from the amorphous BMG phase, the NPD data only provide information about the residual strains in the W fibers. To estimate the stress and strain state in the BMG matrix, a FE model was developed using a commercial software (ABAQUS™). In this model, the fiber stacking was hexagonal to accommodate fiber volume fractions of up to 80% (using a square array of fibers the maximum volume fraction that can be achieved is 78%). Since the fibers had high aspect ratios, a two-dimensional plane strain model was used. General symmetry lines along axes 1 and 2 were enforced by keeping the outer surfaces (the right hand side and the top) as straight lines (see Fig. 6 below). The elements used in the model were eight node, second order, generalized plane strain elements that allow for an overall uniform strain along the longitudinal direction [12]. This way it was possible to determine the elastic strains in all three dimensions. The phase strains (and stresses) were calculated as the volume average of the strains (or stresses) in all the elements composing a given phase. For comparison with the neutron measurements which sample the whole specimen

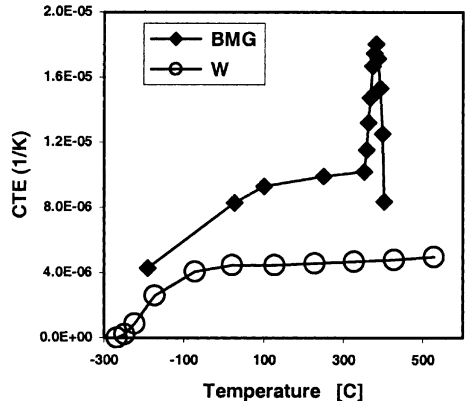

Fig. 3. CTE for W [15] and BMG [13] used in the FE model calculations.

cross-section, the transverse strains, ε_T, were found by averaging the ε_{11} and ε_{22} strain components. The interface between the fibers and the matrix was regarded as intact at all times, an assumption supported by other studies [5]. Both W and BMG are elastically isotropic. In the FE model, they were also considered to be elastic at all temperatures of interest. The material data used in the FE calculations were: for BMG, Young's modulus, $E = 96$ GPa [5], Poisson's ratio, $v = 0.36$ [5], and CTE, $\alpha = 9.0 \times 10^{-6}$–$15 \times 10^{-6}$ K^{-1} [13] (Fig. 3); for W, $E = 410$ GPa [14], $v = 0.28$ [5], $\alpha = 4.5 \times 10^{-6}$–$4.7 \times 10^{-6}$ K^{-1} [15].

Results and discussion

Rietveld refinement revealed a strong $\langle 1\,1\,0 \rangle$ texture along the axis of the W fibers (Fig. 4). Acid etching and scanning electron microscope investigations showed an

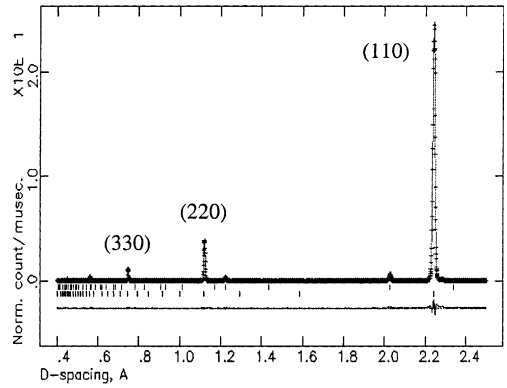

Fig. 4. Diffraction data (normalized intensity vs. d spacing) from the reference W fibers ($2\theta = -90°$). A strong $\langle 1\,1\,0 \rangle$ texture is observed. The second set of tick marks are due to the Al sample holder.

elongated grain structure consistent with the observed texture. This is not surprising given the fact that the fibers were made by wire drawing processes known to induce such texture.

The refinement residuals (R-Bragg) were quite low (~6%) indicating a good fit (Fig. 4). The isotropic atomic displacement, U_{iso}, values obtained from Rietveld analysis ($\sim 2 \times 10^{-3}$–3×10^{-3}) were compared to predictions by the Debye equation [16] and were seen to be in good agreement. To quantify any systematic experimental errors (especially the displacement error in the diffractometer) the 80% W composite was run five times. The results suggest that the uncertainty in the W lattice constant values is within ± 100 με. This number is used for the error bars shown on the neutron strain data in Fig. 5.

The smaller CTE of W is predicted to lead to less contraction in the fibers compared to that in the matrix during cooldown from the processing temperature. As a result, the fibers will be placed in axial compression and transverse tension (on average). The measured average longitudinal and transverse residual strains in W (Fig. 5) follow this expected trend.

In the FE calculations, the effective temperature drop during cooling, ΔT, was adjusted to optimize agreement with the experimental results from the fibers. The magnitude of the predicted W strains was quite sensitive to the value of ΔT and significant changes were observed when ΔT varied by as little as 5°C. This is due to the drastic increase in the CTE of BMG around 350°C (Fig. 3) which is attributed to the amorphous solid BMG alloy becoming an undercooled liquid above this temperature with additional configurational states of lower density [13]. The best fit was found for $\Delta T = 335$°C. This suggests that thermal residual stress buildup started around 355°C (the experiments were carried out at room temperature, $T = 20$°C).

The value of 355°C, perhaps not surprisingly, is near the glass transition of $Zr_{41.2}Ti_{13.8}Cu_{12.5}Ni_{10.}Be_{22.5}$. Waniuk et al. [17] reported that the onset of the glass transition in this alloy is around 352–362°C. It is well known, however, that the glass transition occurs over a temperature range in these BMG alloys and its onset is strongly influenced by the cooling rate during processing [18]. Another important issue is that

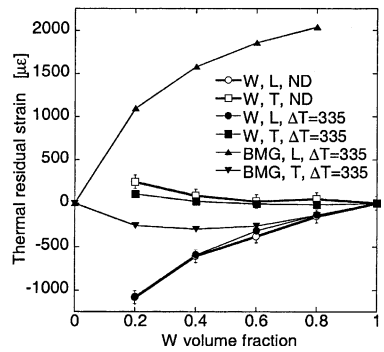

Fig. 5. Comparison of FE calculations (indicated by $\Delta T = 335$) with neutron diffraction (ND) data from W fibers. The strains in the BMG matrix are FE predictions. (L: longitudinal, T: transverse).

material properties change continuously and quickly during the glass transition of BMG alloys. Therefore, although we have assigned a single "freezing" temperature where stress buildup will commence during cooling, its value is likely to be strongly dependent on the exact fabrication conditions.

Nevertheless, our simple, elastic FE model appears to accurately predict the residual stress in the W which suggests that the assumption of elastic behavior of the BMG below its glass transition is plausible. To pursue the validity of this claim, some simple stress relaxation time calculations were performed using the viscosity data for this alloy. Assuming that the viscoelastic behavior of the BMG can be approximated by the Maxwell model, the shear stress relaxation time can be calculated from Ref. [19]: $\tau = \eta/G$, where η is viscosity and G is instantaneous shear modulus (~33 GPa for this alloy [19] and its temperature dependence is neglected). Here, τ is defined as the time it takes an applied shear stress to relax to about 37% (or $1/e$) of its initial value. It is important to note that the viscosity of this alloy changes significantly with time during an isothermal anneal around the glass transition region [17,19]. This is due to its structural relaxation from an amorphous solid to a supercooled liquid during which some of the trapped free volume is relaxed leading to a higher equilibrium viscosity. Therefore, it is impossible to define a single viscosity value at a given temperature around the glass transition. However, the structural relaxation time is usually about two orders of magnitude slower than the shear stress relaxation time [19]. For this reason, the initial viscosity values (before the equilibrium value is reached after structural relaxation) were used in the stress relaxation time calculations. Using the data given in Refs. [17,19], τ values were found to be 2.1 and 0.45 s at 345°C and 365°C, respectively. These results show a rapid change in relaxation time with temperature around the glass transition region for this BMG alloy. These time scales are also reasonable considering the rapid cooling of the composites following melt infiltration. Therefore, the effective "freezing" temperature predicted by the FE calculations (355°C) is a sensible value below which the BMG matrix can be regarded an elastic solid in practice. A more accurate calculation of stress development in composites will require the use of a viscoelastic constitutive relation for the BMG and a detailed temperature history. Such a study is currently underway.

The average residual stresses calculated by the FE model (for $\Delta T = 335$°C) are shown in Table 1. These stresses are significant in both phases and are expected to affect their in situ mechanical behavior during loading. Note that while all stress components in the W fibers are compressive, only the radial stress in the matrix is compressive; both the tangential and longitudinal matrix stresses are tensile. Another important fact is that both radial and tangential stresses in the matrix are maximum at the interface and drop away from it. In comparison to literature data [4,5] for the 40% W/BMG composite, the data in Table 1 show higher stresses. In the former, the calculations were done using the coaxial cylinder model and the longitudinal fiber stress was found to be -200 MPa while the average transverse fiber stress was about -69 MPa. In the matrix, the average values of these stresses were about 130 and 44 MPa, respectively.

Fig. 6 exhibits the distribution of the von Mises stresses, $\sigma_{vM} = \{(\sigma_{11} - \sigma_{22})^2 + (\sigma_{11} - \sigma_{33})^2 + (\sigma_{33} - \sigma_{22})^2\}^{1/2}/\sqrt{2}$, in the 80% W/BMG composite. It is seen that severe

Table 1
Average thermal residual stresses per FE calculations (L: longitudinal, T: transverse)

Fiber volume fraction (%)	BMG		Tungsten	
	σ_L (MPa)	σ_T (MPa)	σ_L (MPa)	σ_T (MPa)
20	130	40	−520	−140
40	200	70	−300	−110
60	250	100	−170	−70
80	300	150	−80	−40

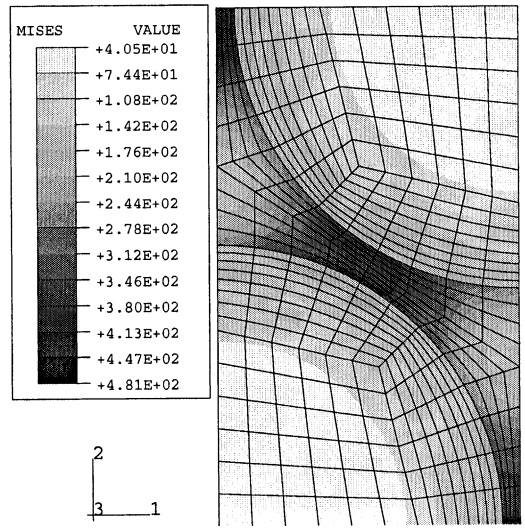

Fig. 6. FE prediction of von Mises stresses (in MPa) in the 80% W/BMG composite. The maximum value of these stresses is over 480 MPa between fibers (dark gray areas).

stress concentrations are predicted in the regions where fibers are closest to each other. These are the areas where shear bands will most likely be initiated.

Conclusions

Neutron diffraction and finite element modeling were used to investigate the thermal residual stresses in W-fiber/BMG–matrix composites. The important findings are:

- The W fibers are severely textured having a $\langle 1\,1\,0 \rangle$ texture along fiber axis.
- An elastic FE model accurately predicts the thermal residual stresses. This suggests that both the fibers and the matrix effectively behave as elastic materials.
- The "freezing" temperature below which residual stress buildup starts during cool-down is near the glass transition temperature of the matrix.

- The residual stresses are significant in both phases. More importantly, there are severe stress concentrations in the matrix between fibers. For instance, maximum von Mises stresses of above 480 MPa were found in the matrix of the 80% W/BMG composite. Such high stresses are expected to strongly influence the mechanical behavior of both phases.

Current work includes the application of stress during neutron diffraction experiments to monitor the in situ mechanical behavior of the W fibers. This way, important information such as the in situ yield stress of the W can be obtained. Another ongoing study is the development of a viscoelastic FE model to more accurately describe the behavior of the BMG matrix.

Acknowledgements

This study was supported by the Army Research Office (grant no. DAAD19-00-1-0379) and the National Science Foundation (CAREER Award 9985264). It also benefited from the national user facility at the Lujan Center (at LANSCE) supported by the US Department of Energy under contract W-7405-ENG-36. Helpful discussions with Professor W.L. Johnson (Caltech) on BMGs and Dr. R.B. von Dreele (LANSCE) on the use of the GSAS program are appreciated.

References

[1] Peker, A., & Johnson, W. L. (1993). Appl Phys Lett 63, 2342.
[2] Gilbert, C. J., Ritchie, R. O., & Johnson, W. L. (1997). Appl Phys Lett 71, 476.
[3] Bruck, H. A., Christman, T., Rosakis, A. J., & Johnson, W. L. (1994). Scripta Metall 30, 429.
[4] Conner, R. D. (1998). Ph.D. Thesis. California Institute of Technology.
[5] Conner, R. D., Dandliker, R. B., & Johnson, W. L. (1998). Acta Mater 46, 6089.
[6] Choi-Yim, H., & Johnson, W. L. (1997). Appl Phys Lett 71, 3808.
[7] Dandliker, R. B., Conner, R. D., & Johnson, W. L. (1998). J Mater Res 13, 2896.
[8] Rietveld, H. M. (1969). J Appl Cryst 2, 65.
[9] Larson, A. C., & Von Dreele, R. B. (1986). GSAS – General Structure Analysis System, LAUR 86-748. Los Alamos National Laboratory.
[10] Young, R. A. (1996). The Rietveld Method. Oxford: Oxford University Press.
[11] Bunge, H. J. (1982). Texture Analysis in Material Science. London: Butterworth.
[12] ABAQUS^{TM}. (1997). Standard User's Manual, (Vol. 57, Section 13.1.2). Pawtucket, RI: Hibbitt, Karlsson and Sorensen.
[13] He, Y., Schwarz, R. B., & Mandrus, D. G. (1996). J Mater Res 11, 1836.
[14] Boyer, H. E., & Gall, T. L. (Eds.). (1985). Metals Handbook, Desk Edition. Metals Park, OH: American Society for Metals.
[15] Touloukian, Y. S., Kirby, R. K., Taylor, R. E., & Desai, P. D. (1975). Thermal Expansion – Thermophysical Properties of Matter, (Vol. 12, p. 354). New York: IFI/Plenum.
[16] Cullity, B. D. (1978). Elements of X-ray Diffraction, 2nd ed. (p. 137). Reading, MA: Addison–Wesley.
[17] Waniuk, T. A., Busch, R., Masuhr, A., & Johnson, W. L. (1998). Acta Mater 46, 5229.
[18] Busch, R., Bakke, E., & Johnson, W. L. (1998). Acta Mater 46, 4725.
[19] Masuhr, A., Waniuk, T. A., Busch, R., & Johnson, W. L. (1999). Phys Rev Lett 82, 2290.